Title

Synthesis of Linkages to Trace Plane Curves

ISBN

978-3-319-56801-0

Authors

Liu, Yang

McCarthy, J Michael

Publication Date

2018

DOI

10.1007/978-3-319-56802-7_26

Synthesis of Linkages to Trace Plane Curves

Yang Liu and J. Michael McCarthy

Abstract Kempe's universality theorem introduced in 1876 has recently been proven to ensure that given any algebraic curve a mechanism exists that traces the curve. In this paper, we present two methods to simplify Kempe's linkages. One method uses gear trains, differentials and belt drives to replace his multiplicator, additor and translator linkages. A second method uses the Scotch yoke mechanism and a summing belt drive to generate a mechanical Fourier series that traces the curve. Examples are provided that demonstrate the two approaches.

1 Introduction

This paper considers the design of a mechanical device that guides a point along a specified curve. The goal is to find a middle ground between the synthesis of linkages using Kempe's construction and the synthesis of linkages using a set of points that approximate the desired curve, called path generation or path synthesis.

Kempe's construction [7] uses a set of standard linkages termed the Reversor, Additor, Multiplicator, and Translator that he combines to constrain the two joint angles of an RR planar chain so its end-point traces a specified algebraic curve. Artobolevskii [2] presents a synthesis theory that yields simpler linkages that trace curves up to degree four.

The approach presented in this paper increases the set of standard linkages used for the synthesis of curve-tracing mechanisms to include gear trains to add and multiply, and pulley and belt drives to translate values. In addition, the desired curve is approximated by its Fourier series representation. The result is physically realizable mechanical devices that trace complex plane curves.

Y. Liu (✉) · J.M. McCarthy
Robotics and Automation Laboratory, University of California, Irvine, CA 92697, USA
e-mail: liuy14@uci.edu

J.M. McCarthy
e-mail: jmmccart@uci.edu

J. Lenarčič and J.-P. Merlet (eds.), *Advances in Robot Kinematics 2016*,
Springer Proceedings in Advanced Robotics 4, DOI 10.1007/978-3-319-56802-7_26

2 Literature Review

Interest in the mechanical generation of plane curves is traced by Nolle [13, 14] and Koetsier [11, 12] to Watt's 1784 patent that describes his approximate straight-line linkage, and the associated parallel motion linkage, which he used in his design of a double acting steam engine; also see Hartenberg and Denavit [4]. In his 1877 book, Kempe [8] summarized the design theory for linkages that generate a straight line, and about the same time presented a construction that yields a linkage to trace a given algebraic curve, see [7].

Kempe's construction introduces a correspondence between linkages and algebraic curves, which has been formalized by Jordan and Steiner [5] and Kapovich and Millson [6], and termed *Kempe's Universality Theorem*. Saxena [17] provides a step-by-step description of this construction to obtain a linkage consisting of 48 links and 70 joints that traces a quadratic curve (Fig. 1). Gao et al. [3] showed that the number of bars in Kempe's construction is of order $O(n^4)$, where n is the degree of algebraic curve. Abbott [1] tightened this bound to $O(n^2)$. However, using the dynamic geometry software Cinderella, Kobel [10] provides a number of examples that illustrate the complexity of the resulting linkages.

Artobolevskii [2] states that the direct application of Kempe's construction "would lead ... to such complicated mechanisms that in practice they would be impossible to achieve." He then proceeds to provide a wide range of practical designs for linkages that generate algebraic curves through degree four and higher. For example, the eight-bar conograph linkage shown in Fig. 2 can be adjusted to trace any quadratic curve.

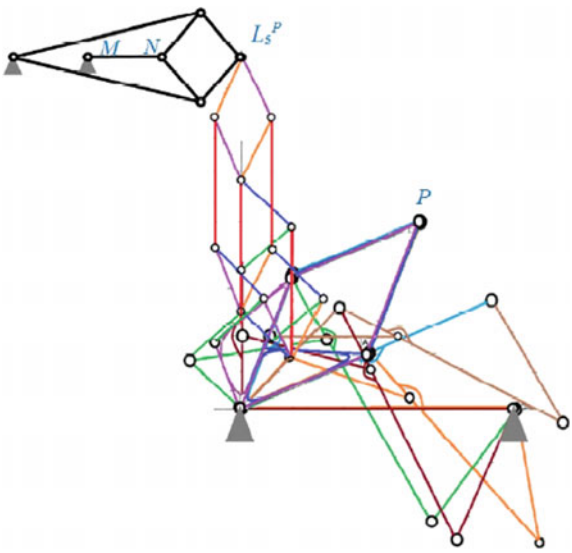

Fig. 1 The linkage that traces the quadratic curve presented in Saxena [17]

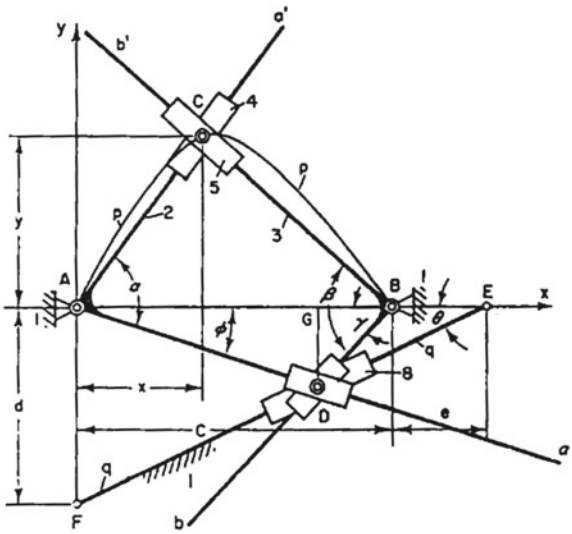

Fig. 2 Artobolevskii [2] shows that this conograph linkage can be adjusted to trace any quadratic plane curve

Roth and Freudenstein [16] introduced a different approach to linkage design for curve tracing. They used the loop equations of a four-bar linkage and nine accuracy points along a desired curve to obtain a system of equations that defined the dimensions of a linkage that guides a coupler point through the given points. Wampler et al. [18] obtained a complete solution for these synthesis equations using polynomial homotopy and showed that there are as many as 4326 distinct four-bar linkages that pass a curve though nine accuracy points. Kim et al. [9] obtained a similar set of synthesis equations for a six-bar linkage and showed that solutions can guide a coupler point though 15 accuracy points. Recent research by Plecnik [15] shows that the equations for 15-point six-bar path generation has a Bezout over 10^{46}, and, while individual solutions can be obtained, it is beyond our ability to compute a complete set of solutions for a given set of 15 accuracy points.

3 Kempe's Linkage with Gears and Pulleys

In this section, we introduce Kempe's method to design planar linkages to trace an algebraic curve. Then we modify his approach to simplify the resulting design.

Let $f(x, y) = 0$ be an algebraic curve. Kempe introduced planar serial chain formed from two revolute joints with link lengths L_1 and L_2 to trace this curve. Thus, the goal is to coordinate the angles θ and ϕ for this RR chain, so that x and y are given by,

$$\mathbf{P} = \begin{Bmatrix} x(\theta, \phi) \\ y(\theta, \phi) \end{Bmatrix} = \begin{Bmatrix} L_1 \cos\theta + L_2 \cos\phi \\ L_1 \sin\theta + L_2 \sin\phi \end{Bmatrix}, \tag{1}$$

such that

$$f(x(\theta, \phi), y(\theta, \phi)) = 0. \tag{2}$$

Kempe shows that this equation can always be reduced to the form,

$$f(\theta, \phi) = \Sigma_i^n A_i \cos(r_i\phi + s_i\theta + \alpha) - C = 0, \tag{3}$$

where $\alpha = 0$ or $\pi/2$, where the A_i and C are constants.

Rather than follow Kempe and introduce his multiplicator, additor, and translator linkages, we use gears, differentials and pulleys to perform these operations. For each r_i and s_i we perform the multiplication using a set of meshing gears, which means for n terms there are at most $g = 2n$ gear pairs. The addition of the terms $r_i\phi + s_i\theta$ are each performed by a gear differential, thus for n terms, we have at most $d = n$ differentials. Finally, we assemble Kempe's serial chain consisting of bars of lengths A_i. We constrain this serial chain to move along the line $x = C$ by a prismatic joint.

In order to obtain the constraint on θ and ϕ to trace the curve f, we connect the gears, differentials and joints of Kempe's serial chain using belts and pulleys. Each pair of gears requires one belt, differential requires two belts, and the n joints of the serial chain requires $n(n + 1)/2$ belts. Finally, three belts are required to drive the RR chain. Thus, the number of belts can be estimated to be,

$$b = g + 2d + n(n + 1)/2 + 3. \tag{4}$$

In order to demonstrate this procedure, we obtain the mechanism that traces the cubic curve,

$$f(x, y) = x^3 - y - 1 = 0. \tag{5}$$

Let $L_1 = L_2 = 1$ be the length of the RR chain that is to trace the curve, and substitute the resulting $x(\theta, \phi)$ and $y(\theta, \phi)$ into to $f(x, y)$ to obtain,

$$f(\theta, \phi) = \cos^3\theta + \cos^3\phi + 3\cos^2\theta\cos\phi + 3\cos^2\phi\cos\theta - \sin\theta - \sin\phi - 1 = 0. \tag{6}$$

The powers of cosine are reduced to first degree using the identities,

$$\cos^2\theta = \frac{1 + \cos(2\theta)}{2}, \quad \cos^3\theta = \frac{3\cos\theta + \cos(3\theta)}{4}. \tag{7}$$

Similarly, the trigonometric sum and difference identities can be used to obtain

$$\begin{aligned} f(\theta, \phi) = {} & \frac{9}{4}\cos\theta + \frac{9}{4}\cos\phi + \frac{1}{4}\cos 3\theta + \frac{1}{4}\cos 3\phi + \frac{3}{4}\cos(2\theta - \phi) + \frac{3}{4}\cos(2\theta + \phi) \\ & + \frac{3}{4}\cos(2\phi - \theta) + \frac{3}{4}\cos(2\phi + \theta) + \cos(\frac{\pi}{2} + \theta) + \cos(\frac{\pi}{2} + \phi) = 1, \end{aligned} \tag{8}$$

which has $n = 10$ terms.

Table 1 Serial chain configuration

Link number	Link length	Phase offset (Degree)	Angular velocity
A_1	2.25	−60	θ
A_2	2.25	60	ϕ
A_3	0.25	−180	3θ
A_4	0.25	180	3ϕ
A_5	0.75	−180	$2\theta - \phi$
A_6	0.75	−60	$2\theta + \phi$
A_7	0.75	180	$2\phi - \theta$
A_8	0.75	60	$2\phi + \theta$
A_9	1	30	θ
A_{10}	1	150	ϕ

Examining (8) we see that Kempe's serial chain that constrains θ and ϕ has 10 links, which are listed in Table 1. This equation requires six gear pairs and four differentials. The number of belts are computed to be 72.

The initial configuration of the links in Kempe's serial chain can be determined by setting the initial position of $\mathbf{P} = (1, 0)$, so we have

$$\begin{Bmatrix} 1 \\ 0 \end{Bmatrix} = \begin{Bmatrix} \cos\theta + \cos\phi \\ \sin\theta + \sin\phi \end{Bmatrix}. \tag{9}$$

Solve this equation to obtain

$$\begin{aligned} \theta &= -60^\circ, \quad \phi = 60^\circ, \\ \theta &= 60^\circ, \quad \phi = -60^\circ. \end{aligned} \tag{10}$$

Both solutions work, so we pick the first solution. This defines each of the angles of the links in the Kempe's serial chain, see Table 1. This mechanical system traces the algebraic curve when the end of Kempe's serial chain is constrained to move along the line $x = 1$ by a prismatic joint, Fig. 3.

In order to compare our linkage to Kempe's construction, we count the components of elementary versions of Kempe's additor, multiplicator and translator linkages. The additor has six bars and is required for each addition including the constants. A multiplication by k requires a multiplicator with at least $m(k) = 2(k-2) + 6$ bars. We model the translator as a parallelogram linkage that requires three bars for each belt used in our design, which means t = 3b. Therefore, in order to estimate Kempe's linkage, we note that (8), requires $a = 6$ additors, $m(2) = 4$ multiplicators with $k = 2$, and $m(3) = 2$ with $k = 3$, thus

$$p = 6a + m(2)6 + m(3)8 + 3b = 36 + 24 + 16 + 216 = 292. \tag{11}$$

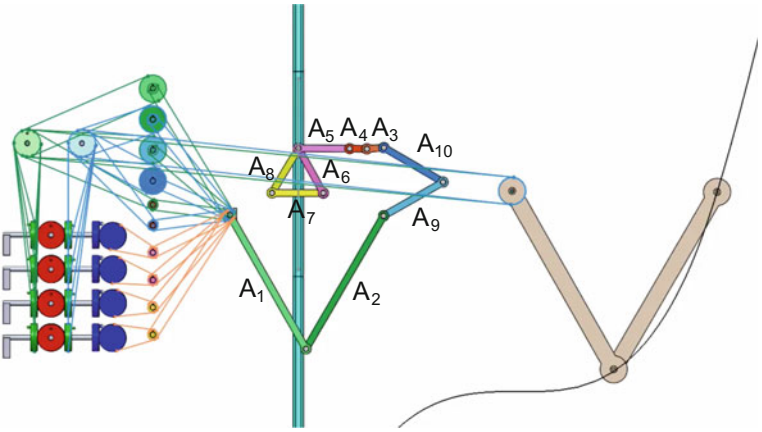

Fig. 3 Gear pairs, differentials and belt drives are used to provide the multiplications, additions and transmission necessary to constrain the RR chain to trace this curve

Thus, we can estimate Kempe's construction to require at least 292 parts for this example.

If we count the individual parts for our method, we have two gears per multiplication and four gears per addition, and two pulleys for each belt. Thus, the part count is

$$p = 2g + 4d + 2b + b = 12 + 15 + 144 + 72 = 244. \tag{12}$$

This comparison shows that the primary difference arises from the complexity of the multiplicator linkage. Our method simplifies this further by using the sizes of pulleys to perform the multiplication. This also shows the dominant role that the translator linkages play in the part count of Kempe's designs. It is our expectation that effective use of gears, differentials, belts and pulleys can simplify the application of Kempe's results to a wide range of algebraic curves.

4 Fourier Series Method

In this section, we provide another approach to the design of a mechanism to trace a plane curve. We assume the curve can be parameterized, then we compute its Fourier decomposition for each component function. We use an array of Scotch yoke mechanisms to generate individual terms and use a belt to add the terms of the Fourier series.

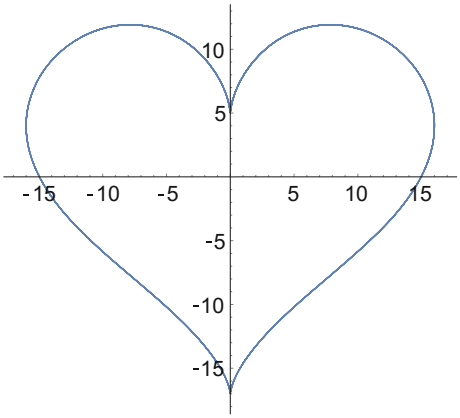

Fig. 4 The parameterized heart curve has a finite Fourier expansion for each coordinate function

In order to demonstrate this procedure, we obtain a mechanism that traces the heart curve (Fig. 4),

$$\begin{Bmatrix} x \\ y \end{Bmatrix} = \begin{Bmatrix} 16\sin^3 t \\ 13\cos t - 5\cos 2t - 2\cos 3t - \cos 4t \end{Bmatrix}. \tag{13}$$

Now reduce powers of sine to first degree using the identity,

$$\sin^3\theta = \frac{3\sin\theta - \sin 3\theta}{4} \tag{14}$$

The result is the equation,

$$\begin{Bmatrix} x \\ y \end{Bmatrix} = \begin{Bmatrix} 12\sin t - 4\sin 3t \\ 13\cos t - 5\cos 2t - 2\cos 3t - \cos 4t \end{Bmatrix}. \tag{15}$$

Reduce minus sign using shift angle properties of trigonometric function, and convert sine terms into cosine terms to obtain

$$\begin{Bmatrix} x \\ y \end{Bmatrix} = \begin{Bmatrix} 12\cos(\frac{-\pi}{2} + t) + 4\cos(\frac{-3\pi}{2} + 3t) \\ 13\cos t + 5\cos(\pi + 2t) + 2\cos(\pi + 3t) + \cos(\pi + 4t) \end{Bmatrix}. \tag{16}$$

The mechanical system that traces this heart curve is obtained by using two Scotch yoke mechanisms for the two terms of the x coordinate, and four of these mechanisms for the y coordinate. These terms are summed using belts. See Fig. 5.

This mechanism provides another approach to the design of mechanisms to trace a plane curve. We have also used this Fourier series approach to design a curve that fits an image generated by an array of points.

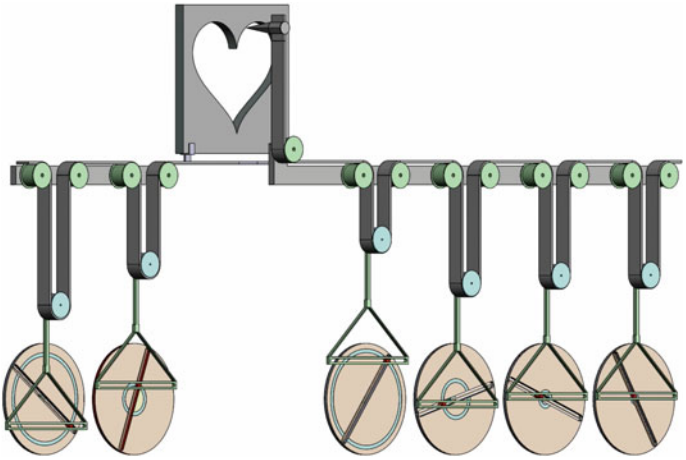

Fig. 5 Each Scotch yoke mechanism computes a term in the Fourier expansion of the x and y coordinate functions for the heart curve. There are two terms for x component and four terms for the y component

5 Conclusion

In this paper, we present two ways to assemble a mechanical system to trace plane curves. The first method uses Kempe's universality theorem that guarantees a mechanism exists for any algebraic plane curve. We use gear pairs, differentials and belt drives to simplify the resulting device. The second method uses a mechanical Fourier series constructed from Scotch yoke mechanisms to generate a parametrized plane curve. Kempe's formulation provides an exact representation of algebraic curves, while the Fourier formulation is exact for certain parameterized curves. These are early results in the formulation of a design methodology for mechanical systems that trace arbitrary plane curves.

References

1. Abbott, T.G.: Generalizations of Kempe's Universality Theorem. Massachusetts Institute of Technology (2008)
2. Artobolevskii, I.I.: Mechanisms for the Generation of Plane Curves. Pergamon Press, New York (1964)
3. Gao, X.S., Zhu, C.C., Chou, S.C., Ge, J.X.: Automated generation of Kempe linkages for algebraic curves and surfaces. Mech. Mach. Theory **36**, 1019–1033 (2001)
4. Hartenberg, R.S., Denavit, J.: Kinematic Synthesis of Linkages. McGraw-Hill, New York (1964)
5. Jordan, D., Steiner, M.: Configuration spaces of mechanical linkages. Discret. Comput. Geom. **22**, 297–315 (1999)

6. Kapovich, M., Millson, J.J.: Universality theorems for configuration spaces of planar linkages. Topology **41**(6), 1051–1107 (2002)
7. Kempe, A.B.: On a general method of describing plane curves of the nth degree by linkwork. Proc. Lond. Math. Soc. **VII**(102), 213–216 (1876)
8. Kempe, A.B.: How to Draw a Straight Line. Macmillan and Co, London (1877)
9. Kim, H.S., Hamid, S., Soni, A.H.: Synthesis of six-link mechanisms for point path generation. J. Mech. **6**, 447–461 (1971)
10. Kobel, A.: Automated generation of Kempe linkages for algebraic curves in a dynamic geometry system. Saarland University, Saarbrucken, Germany, Faculty of Natural Sciences and Technology, Department of Computer Science (2008)
11. Koetsier, T.: A contribution to the history of kinematics-i, Watt's straight-line linkages and the early French contributions to the theory of the planar 4-bar coupler curve. Mech. Mach. Theory **18**(1), 37–42 (1983)
12. Koetsier, T.: A contribution to the history of kinematics-ii, the work of English mathematicians on linkages during the period 1869–1878. Mech. Mach. Theory **18**(1), 43–48 (1983)
13. Nolle, H.: Linkage coupler curve synthesis: a historical review-i. Developments up to 1875. Mech. Mach. Theory **9**, 147–168 (1974)
14. Nolle, H.: Linkage coupler curve synthesis: a historical review-ii. Developments after 1875. Mech. Mach. Theory **9**, 325–348 (1974)
15. Plecnik, M.M.: Dimensional synthesis of six-bar linkages for function, motion and path synthesis. Ph.D. thesis, University of California, Irvine (2015)
16. Roth, B., Freudenstein, F.: Synthesis of path-generating mechanisms by numerical methods. J. Eng. Ind. **85**, 298–304 (August 1963)
17. Saxena, A.: Kempe's linkages and the universality theorem. Resonance **16**, 220–237 (March 2011)
18. Wampler, C.W., Morgan, A.P., Sommese, A.J.: Complete solution of the nine-point path synthesis problem for four-bar linkages. J. Mech. Des. **114**, 153–159 (1992)

Subject-Specific Model of Knee Natural Motion: A Non-invasive Approach

Michele Conconi, Nicola Sancisi and Vincenzo Parenti-Castelli

Abstract The capability to model human joint motion is a fundamental step towards the definition of effective treatments and medical devices, with an increasing request to adapt the devised models to the specificity of each subject. We present a new approach for the definition of subject-specific models of the knee natural motion. The approach is the result of a combination of two different techniques and exploits the advantages of both. It relays upon non invasive measurements based on which a kinematic model of the natural motion is built, suitable to be extended to the definition of static and dynamic models. Comparison of the model outcomes with in vitro measurements performed on one specimen shows promising results supporting the proposed approach.

1 Introduction

The natural motion of the knee is the motion of the joint in unloaded conditions. It is the joint starting condition before loads are applied, thus contributing in the determination of the tibio-femoral relative position in loaded conditions. For this reason, the knowledge of the natural motion is useful for all applications which aim at replicating or restoring the natural behaviour of the knee, such as lower-limb modelling, surgical planning and prosthesis design.

The modelling of the joint natural motion can be based on mean data taken from the literature, thus providing a representation of an average joint [3, 17, 24]. However, there is an increasing request of subject-specific models that would allow personalization of treatments and prosthesis geometry to the patient needs. In these cases, the subject-specific motion would be required.

M. Conconi (✉) · N. Sancisi · V. Parenti-Castelli
DIN - Department of Industrial Engineering, University of Bologna, Bologna, Italy
e-mail: michele.conconi@unibo.it

N. Sancisi
e-mail: nicola.sancisi@unibo.it

V. Parenti-Castelli
e-mail: vincenzo.parenti@unibo.it

J. Lenarčič and J.-P. Merlet (eds.), *Advances in Robot Kinematics 2016*,
Springer Proceedings in Advanced Robotics 4, DOI 10.1007/978-3-319-56802-7_27

An accurate estimation of the joint motion is difficult to obtain in vivo [16]: non-invasive techniques could be inaccurate (skin-markers) or too complicated (fluoroscopy) for standard practice, while more invasive techniques (bone-pins) are not acceptable in most cases. Thus, new solutions are needed to predict the joint motion with a good accuracy, based on non-invasive measurements.

In this study a new approach is presented which exploits two techniques with complementary advantages for the modelling of the knee natural motion. The first technique (T1), was originally developed and validated for the ankle joint [4] and is here tested on the knee. T1 predicts the joint motion by optimizing the articular load distribution, assuming this condition as representative of the joint behaviour in physiological working conditions. T1 only requires a 3D representation of the articular surfaces that can be obtained from standard in vivo images of the articulation. It is however not suitable for the characterization of the joint behaviour under generic working conditions.

The second technique (T2) models the knee as a one-degree-of-freedom (1-Dof) spatial mechanism, featuring the two articular contacts and the three isometric fibres of the anterior cruciate (ACL), posterior cruciate (PCL) and medial collateral (MCL) ligaments [17, 18]. T2 was very accurate to replicate the natural motion of specimens over the full flexion arc and can be easily extended to define more complex static and dynamic models that can take into account different loading conditions [22, 23], but a reference motion is needed to adjust the model parameters.

In this study we want to exploit the advantages of both techniques by combining them into a new approach (T1+T2) which allows the definition of subject-specific models of the knee (as T2 does) from non invasive observations of its natural motion (via T1).

The aim of this work is twofold: first, to evaluate the application of T1 to the knee articulation and, second, to test the applicability of T1+T2 on the same joint. To this purpose, a leg specimen is analyzed and the knee joint motion is obtained by T1 starting from magnetic resonance imaging (MRI) data. The motion resulting from T1, together with additional information about the anatomy of the joint specimen also taken from MRI, is used as an input for the definition of T2. Finally, the results of both T1 and T1+T2 are validated against in vitro experimental measurements of the joint natural motion.

2 Materials and Methods

2.1 T1 Technique

Biologic tissues are able to modify their structure in response to the mechanical environment to which they are exposed [2, 6, 12, 19]. Experimental evidence from the literature suggests that the aim of this process is the mechanical optimization of the tissues (functional adaptation). In particular, this process produces articular surfaces

that, in physiological working conditions, optimize the contact load distribution or, equivalently, maximize the joint congruence [8, 13].

It is thus possible to identify the adapted motion as the envelope of the maximum congruence configurations (i.e., positions and orientations of all bones constituting the joint). In [5] a measure of joint congruence was proposed, based on the Winkler elastic foundation contact model [14]. This measure makes it possible to estimate the peak-pressure to resultant-force ratio from the geometry of the articulating surfaces at a given configuration, i.e., from a purely geometrical perspective. As a consequence, the adapted motion can be obtained starting solely from the knowledge of the shape of the articular surfaces.

As discussed in [4], the adapted motion should also keep the isometry of the joint main ligaments. This condition is verified during the natural motion, which for this reason can be taken as a good approximation of the adapted one. In the same study, T1 was used to determine the adapted motion of ten human ankles, providing good agreement with experimental measurements of the natural motion of the same specimens. Based on these results, T1 is here applied to determine the knee natural motion.

2.2 T2 Technique

Many studies showed that the natural motion of the tibia with respect to the femur is represented by a complex 1-Dof spatial path, i.e. the relative position and orientation of the tibia and femur is a function of a single motion parameter, for instance the flexion angle [17, 24]. Moreover, some fibres of the ACL, PCL and MCL proved to be almost isometric during this motion. From a mechanical point of view, this means that the natural motion can be reproduced by an appropriate 1-Dof mechanism. Three-dimensional parallel mechanisms were thus defined based on this concept. One of them [17, 18] featured three rigid links representing the ACL, PCL and MCL, while the contacts between tibial and femoral condyles were replaced by the contacts between two pairs of spheres, or, equivalently, by two rigid links connecting the sphere centres at each pair. The result was a 1-Dof 5-5 spatial parallel mechanism, which features two rigid bodies (the femur and tibia) interconnected by 5 binary links.

In previous studies, the initial geometry of the mechanism, namely the attaching points and lengths of the five rigid links was determined from knee specimens. This initial geometry was then optimized in order to best-fit the experimental natural motion of the corresponding specimens [22]. This approach has been extensively validated with very good agreement between model outcomes and corresponding experimental natural motion [17]. The same approach is applied here, but the motion obtained by T1 is used as a reference for the model definition instead of the subject experimental motion.

2.3 Data Acquisition and Processing

A single fresh-frozen lower-limb specimen from a donor (female, 63 years old, weight 68 kg, height 158 cm) was analyzed. The study was approved by the donor organization, which provided written consent. A surgeon declared the leg free from anatomical defects and removed the forefoot and the soft tissues external to the joint, leaving the knee joint capsule and ligaments intact.

A stereophotogrammetric system (Vicon Motion Systems Ltd) was used to measure the tibia and femur relative motion by means of two trackers directly fixed to the bones, thus introducing no soft tissue artefacts (Fig. 1a). The specimen was mounted on a test rig for in vitro analysis of the knee joint behaviour [7] which also allows measurement of the femur-tibia relative motion when no external forces are applied. In this condition, the joint is guided only by the knee passive structures, namely ligaments and contacts, and thus the natural motion can be registered. This experimental natural motion was used only for validation purposes, but it was not used for model definition.

A MRI of the knee was acquired using an isotropic three-dimensional fast spin-echo pulse sequence T2-weighted (3D-FSE-CUBE-T2) within a 1.5 T scanner. Articular surfaces and ligament insertions were then manually segmented using the free open-source software Medical Imaging Interaction Toolkit (MITK), obtaining 3D models of the femur and tibia including bone, cartilage and ligaments (Fig. 1b). In the same way, anatomical reperi were determined on the femur and tibia models, and were used to build anatomical reference systems [22] on both bones (Fig. 2).

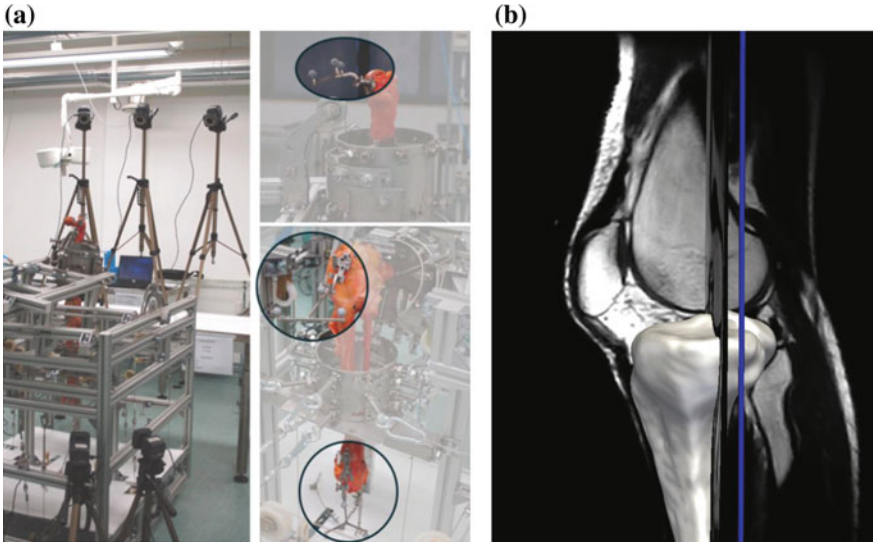

Fig. 1 **a** Stereophotogrammetric system for the measure of the bone relative motion. **b** Reconstruction of knee anatomy from MRI

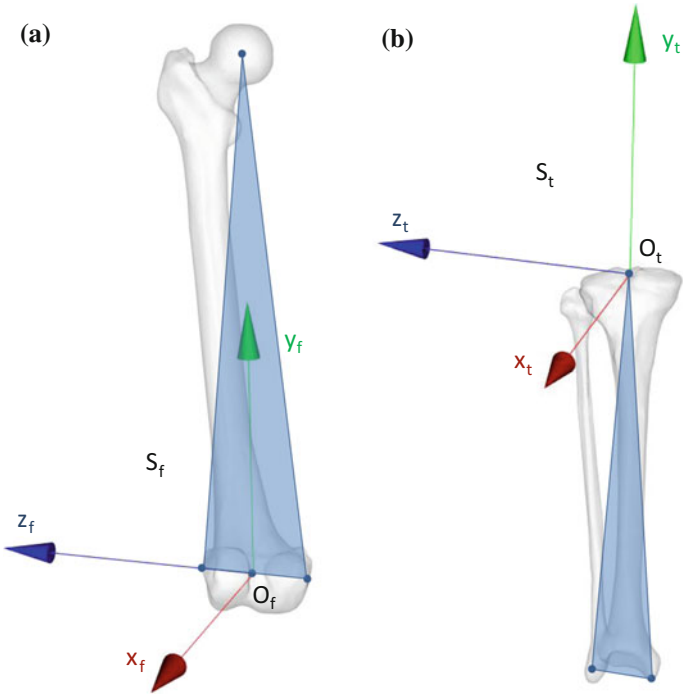

Fig. 2 Anatomical reference systems for the femur **a** and the tibia **b**. The tibia anatomical frame has origin in the tibia centre, i.e., the deepest point in the sulcus between the medial and lateral tibial intercondylar tubercles; x-axis orthogonal to the plane defined by the two malleoli and the tibia centre, anteriorly directed; y-axis directed from the midpoint between the malleoli to the tibia centre; z-axis as a consequence, according to the right hand rule. The femur anatomical frame has origin in the midpoint between the lateral and medial epicondyles; x-axis orthogonal to the plane defined by the two epicondyles and the hip joint centre, anteriorly directed; y-axis directed from the origin to the hip joint centre; z-axis as a consequence, according to the right hand rule

The relative motion of these reference systems was then expressed by means of a standard convention [10], both for the computed and experimental motions.

The anatomical 3D models of the femur and tibia, comprehensive of both bone and articular cartilage, were used within T1 for the evaluation of the knee joint congruence. Flexion angle was imposed and the other five motion components were obtained by maximizing the congruence; the procedure was repeated over the full flexion arc [4].

T2 definition was then performed based on the T1 motion and on the 3D femur and tibia models. The articular surfaces at the femur condyles and tibia plateaus used for congruence evaluation in T1 were approximated by best-fitting spheres in T2, and were then substituted by equivalent rigid links connecting the sphere centres. The most isometric fascicles of the ACL, PCL, MCL (i.e., the anteromedial, posteromedial, anterior fascicle respectively) were identified within the segmented

ligament insertion areas [11]. The ligament isometric fibres were obtained as the pair of points (one on the femur, the other on the tibia insertion areas of isometric fascicles) that showed the minimum change in distance during the motion obtained by T1. The so-determined isometric fibres were then substituted by three rigid links. Finally, these preliminary mechanism parameters were adjusted by an optimization procedure [22] to best-fit the T1 motion. The final mechanism parameters were constrained to remain inside the experimental insertion areas and to have a maximum distance of 2 mm with respect to the preliminary parameters.

3 Results

The relative motion of the tibia and femur identified by T1 was consistent with the joint constraints. All ligaments indeed showed very small length changes during T1 motion: isometric fibre length excursions were smaller than 4% of the relevant fibre maximum length for the ACL, PCL, MCL and the lateral collateral ligament (LCL), in agreement with what reported in the literature [1]. The subsequent application of T2 made the ACL, PCL, MCL perfectly isometric, while the LCL showed a length change smaller than 2%. Figure 3 shows the add-abduction (AA), the in-external rotation (IE) and the antero-posterior (AP), proximo-distal (PD) and medio-lateral (ML) translation of the tibia, plotted versus the knee flexion angle as experimentally measured and computed by T1 and T1+T2.

In Table 1, the mean absolute errors (MAE) between T1 and experimental natural motions, between T1+T2 and T1 motions and between T1+T2 and experimental natural motions are presented.

4 Discussion

The tibio-femoral motion predicted by the combination of the two techniques T1 and T2 well replicates the experimental data. There are however some differences in the IE rotation and AP translation, for which the MAEs between the model and the natural motion are about 12 and 4.5 mm, respectively. Despite these quantitative differences, computed and experimental curves show a very similar trend, in particular for the IE rotations which differ essentially by a constant offset. The typical screw-home motion of the knee is therefore correctly predicted by the model, but at each flexion angle the configuration of the tibia results less internally rotated than in the natural motion.

It is worth mentioning that, despite ligaments and contacts do guide the knee natural motion on a 1-Dof spatial path, the IE rotation is less constrained than the other motion components. As a result, the knee shows the smallest stiffness about the IE axis [9, 15], which is thus the most sensitive among the knee motion components both for experimental measure and for numerical models. For what concern the AP

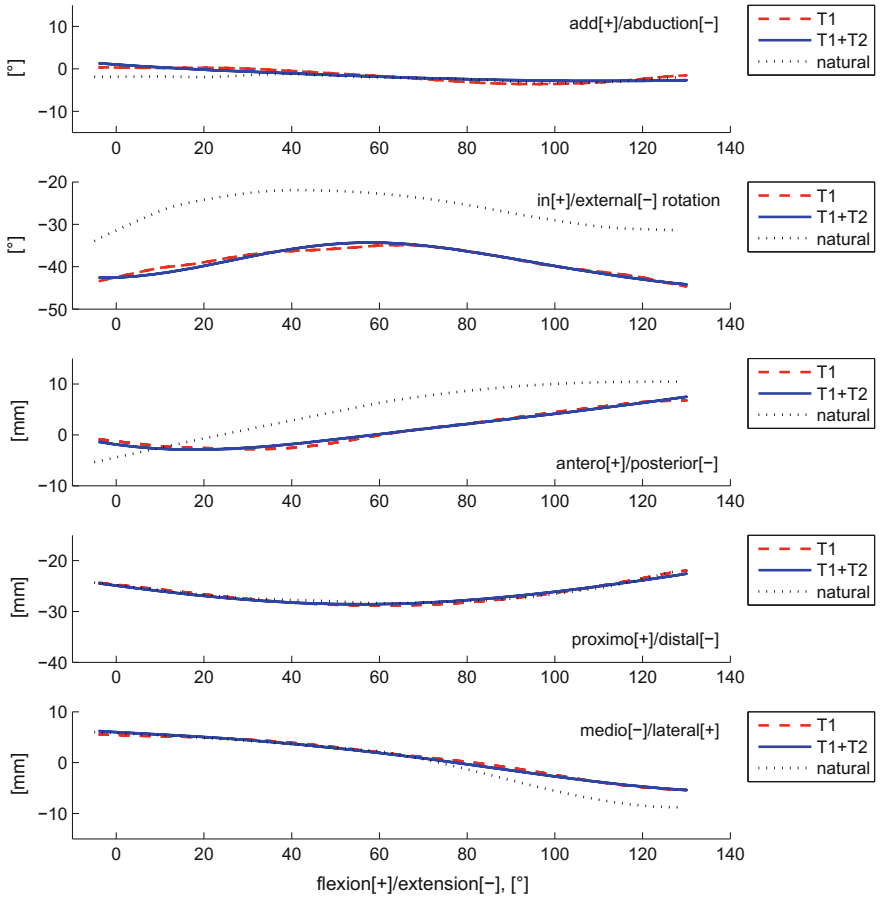

Fig. 3 Tibio-femoral relative motion as resulting from T1 (*red dashed*), T1+T2 (*blue continue*) and experimental natural motion (*black dotted*)

Table 1 MAE for each motion component between T1 and experimental motion, between T1+T2 and T1 motion and between T1+T2 and experimental motion

	AA [°]	IE [°]	AP [mm]	PD [mm]	ML [mm]
T1 versus exp.	0.90	12.24	4.55	0.32	1.22
T1+T2 versus T1	0.54	0.64	0.34	0.28	0.26
T1+T2 versus exp.	0.79	12.43	4.55	0.33	1.19

translations, variations in the IE rotation of the tibia are associated with AP displacements of the same bone. In fact, the tibiofemoral motion is close to a spherical one [21], whose centre does not coincide with the centre of the tibial anatomical reference system. As a result, an IE rotation of the tibia is associated with a translation of the

origin of its reference system, mainly along the AP direction. It is thus reasonable that differences in the IE rotation are associated with differences in the AP translation.

Despite the above mentioned differences, both the motion computed by T1 and the experimental natural one respects the ligament isometry, producing length changes smaller than 4 and 5% respectively for the ACL, PCL, MCL and LCL. This result supports the analogy between adapted and natural motion, as validated for the ankle [4] and here hypothesized for the knee. It should also be stressed that only the ligament isometry during the T1 motion made it possible the subsequent application of T2. In fact, in general it is not possible to define a 5-5 mechanism that both follows a generic prescribed path and respects the joint anatomical constraints at the same time. A wider validation of T1 is therefore necessary in order to fully understand the relation between the natural and adapted motion of the knee joint, in terms of both the differences and analogies in terms of motion and ligament isometric behaviour shown in this study.

A similar combination of T1 and T2 was investigated in [20]. In that case however, only CT images of the knee were available, thus providing poor accuracy in the reconstruction of soft tissues that introduced some noise in the motion computed by T1. These limitations were overcome in this study by means of MRI of the articular surfaces. Moreover, the use of MRI makes the proposed approach less invasive with respect to CT images, not exposing the patient to ionizing radiation, and therefore more suitable for the in vivo clinical application.

5 Conclusion

The aim of this study was to test a new approach for the generation of subject-specific model of the natural motion of the knee joint based on non invasive measurements. This approach relays on two techniques defined as T1 and T2 that contribute to determine the final model. The advantages of both techniques are exploited: T1 provides an evaluation of the knee natural motion by non invasive measurements of the articular surfaces; then, based on this motion, T2 provides a mechanism which complies with the constraints imposed by the ligaments and articular contacts, and that can be easily extended to define more complex static and dynamic models.

The motion resulting from T1 fulfils the ligament isometry typical of the knee natural motion, thus making it possible the subsequent application of T2. The results of the combination of T1 and T2 are in good agreement with experimental data, although some differences were found.

Future work is therefore in progress on other specimens in order to further validate the proposed approach and to investigate whether the observed differences are common to all the knee joints, and in case to give a solid explanation of them.

References

1. Belvedere, C., Ensini, A., Feliciangeli, A., Cenni, F., D'Angeli, V., Giannini, S., Leardini, A.: Geometrical changes of knee ligaments and patellar tendon during passive flexion. J. Biomech. **45**(11), 1886–1892 (2012)
2. Benjamin, M., Ralphs, J.R.: Fibrocartilage in tendons and ligaments-an adaptation to compressive load. J. Anat. **193**(Pt 4), 481–494 (1998)
3. Blankevoort, L., Huiskes, R., De Lange, A.: The envelope of passive knee joint motion. J. Biomech. **21**(9), 705–720 (1988)
4. Conconi, M., Leardini, A., Parenti-Castelli, V.: Joint kinematics from functional adaptation: A validation on the tibio-talar articulation. J. Biomech. **48**(12), 2960–2967 (2015)
5. Conconi, M., Parenti-Castelli, V.: A sound and efficient measure of joint congruence. Proc. Inst. Mech. Eng. Part H J. Eng. Med. **228**(9), 935–941 (2014)
6. Eckstein, F., Hudelmaier, M., Putz, R.: The effects of exercise on human articular cartilage. J. Anat. **208**, 491–512 (2006)
7. Forlani, M., Sancisi, N., Conconi, M., Parenti-Castelli, V.: A new test rig for static and dynamic evaluation of knee motion based on a cable-driven parallel manipulator loading system. Meccanica (2015). doi:10.1007/s11012-015-0124-1
8. Frost, H.M.: An approach to estimating bone and joint loads and muscle strength in living subjects and skeletal remains. Am. J. Hum. Biol. **11**, 437–455 (1999)
9. Grood, E.S., Stowers, S.F., Noyes, F.R.: Limits of movement in the human knee. Effect of sectioning the posterior cruciate ligament and posterolateral structures. J. Bone Joint Surg. Am. **70**(1), 88–97 (1988)
10. Grood, E.S., Suntay, W.J.: A joint coordinate systenf for the clinical description of three-dimensional motions: application to the knee. J. Biomech. Eng. **135**, 136–144 (1983)
11. Harner, C.D., Baek, G.H., Vogrin, T.M., Carlin, G.J., Kashiwaguchi, S., Woo, S.L.: Quantitative analysis of human cruciate ligament insertions. Arthrosc. J. Arthrosc. Relat. Surg. **15**(7), 741–749 (1999)
12. Hayashi, K.: Biomechanical studies of the remodeling of knee joint tendons and ligaments. J.Biomech. **29**, 707–716 (1996)
13. Heegaard, J.H., Beaupre, G.S., Carter, D.R.: Mechanically modulated cartilage growth may regulate joint surface morphogenesis. J. Orthop. Res. **17**, 509–517 (1999)
14. Johnson, K.: Contact Mechanics. Cambridge University Press, Cambridge (1985)
15. Markolf, K.L., Mensch, J.S., Amstutz, H.C.: Stiffness and laxity of the knee-the contributions of the supporting structures. A quantitative in vitro study. J. Bone Joint Surg. Am. **58**(5), 583–594 (1976)
16. Masum, M.A., Pickering, M.R., Lambert, A.J., Scarvell, J.M., Smith, P.N.: A review: techniques for kinematic analysis of knee joints. In: Australian Biomedical Engineering Conference (ABEC) (2014)
17. Ottoboni, A., Parenti-Castelli, V., Sancisi, N., Belvedere, C., Leardini, A.: Articular surface approximation in equivalent spatial parallel mechanism models of the human knee joint. Proc. Inst. Mech. Eng. Part H J. Eng. Med. **224**(9), 1121–1132 (2010)
18. Parenti-Castelli, V., Di Gregorio, R.: Parallel mechanisms applied to the human knee passive motion simulation, pp. 333–344. Kluwer Academic Publishers, Pirano-Portoroz, Slovenia (2000)
19. Robling, A.G., Castillo, A.B., Turner, C.H.: Biomechanical and molecular regulation of bone remodeling. Ann. Rev. Biomed. Eng. **8**, 455–498 (2006)
20. Sancisi, N., Conconi, M., Parenti-Castelli, V.: Prediction of the subject-specific knee passive motion from non-invasive measurements. In: The 25th Congress of the International Society of Biomechanics - XXV ISB. Glasgow, UK (2015)
21. Sancisi, N., Parenti-Castelli, V.: A 1-dof parallel spherical wrist for the modelling of the knee passive motion. Mech. Mach. Theory **45**(4), 658–665 (2010)

22. Sancisi, N., Parenti-Castelli, V.: A novel 3d parallel mechanism for the passive motion simulation of the patella-femur-tibia complex. Meccanica **46**(1), 207–220 (2011)
23. Sancisi, N., Parenti-Castelli, V.: On the role of passive structures in the knee loaded motion, pp. 1–8. Springer, Berlin (2012)
24. Wilson, D., Feikes, J., Zavatsky, A., O'Connor, J.: The components of passive knee movement are coupled to flexion angle. J. Biomech. **33**(4), 465–473 (2000)

Springer Proceedings in Advanced Robotics 4
Series Editors: Bruno Siciliano · Oussama Khatib

Jadran Lenarčič
Jean-Pierre Merlet *Editors*

Advances in Robot Kinematics 2016

spar

Springer

Springer Proceedings in Advanced Robotics 4

Jadran Lenarčič · Jean-Pierre Merlet
Editors

Advances in Robot Kinematics 2016

Springer

Editors
Jadran Lenarčič
Jožef Stefan Institute
Ljubljana
Slovenia

Jean-Pierre Merlet
INRIA Sophia Antipolis
Sophia Antipolis Cedex
France

ISSN 2511-1256 ISSN 2511-1264 (electronic)
Springer Proceedings in Advanced Robotics
ISBN 978-3-319-56801-0 ISBN 978-3-319-56802-7 (eBook)
DOI 10.1007/978-3-319-56802-7

Library of Congress Control Number: 2017940802

Printed on acid-free paper

This Springer imprint is published by Springer Nature
The registered company is Springer International Publishing AG
The registered company address is: Gewerbestrasse 11, 6330 Cham, Switzerland